Proc. R. Soc. Lond. B. **201**, 131–147 (1978)
Printed in Great Britain

The photoreceptors and pigment epithelium of the adult *Xenopus* retina: morphology and outer segment renewal

By Marion S. Kinney† and S. K. Fisher

Department of Biological Sciences, University of California, Santa Barbara, California 93106 *U.S.A.*

(*Communicated by B. B. Boycott, F.R.S. – Received* 27 *July* 1977)

[Plates 1–6]

Outer segment renewal and the fine structure of photoreceptors and pigment epithelium (p.e.) were studied in the adult *Xenopus* retina by light microscopic autoradiography and electron microscopy. Following the injection of [^{3}H]leucine, the pattern of labelling observed in receptor outer segments was typical of that reported in other adult retinae: only diffuse labelling was found in cones, but in rods a discrete band of label accumulated at the base of the outer segment and migrated sclerally with time. The rate of band displacement and thus disk addition in *Xenopus* rods was 1.86 μm/day (or 78 disks/day), which is more than twice that reported for red rods in *Rana* under similar experimental conditions, although these species have similar metabolic rates. Average rod outer segment (r.o.s.) length did not change, demonstrating a balance between disk addition and shedding. R.o.s. renewal time was about 24 days, corresponding to the time when labelled phagosomes were first found in the p.e. Ultrastructurally, one kind of (red) rod and one kind of cone were found whose outer segments differed in membrane topology. Although microfilaments were found in the apical processes of the p.e. and its cytoplasm contained both pigment granules and myeloid bodies, pigment granules did not migrate into these processes during light adaptation. In addition to possible morphological evidence for phagosomes of cone origin, both large and small rod phagosomes were observed in the p.e. The latter appear to represent small stacks of partial disks shed from individual r.o.s. scallops.

Introduction

The process by which vertebrate photoreceptors renew their membranous outer segments was first discovered by autoradiographic studies about ten years ago by Young (Young 1967; Young & Droz 1968; for a review see Young 1976). Following injection of radioactive amino acids, a distinct band of radioactive material accumulates at the base of each rod outer segment (r.o.s.) and migrates sclerally with time (Young 1967). Electron microscopic evidence (Young & Droz 1968) supports the conclusion that in rods, protein synthesized from amino acids

† Present address: Department of Physiology, University of California, San Francisco, California 94143, U.S.A.

in the inner segment is transported through the connecting cilium to the outer segment, where it is assembled into new disk-membrane forming by invagination of the outer segment base. These membranes soon lose continuity with the outer plasma membrane by pinching off as individual discs (Hall, Bok & Bacharach 1969), thus trapping the protein molecules within separate disks (Young 1974). Biochemical analysis of r.o.s. reveals that most of the radioactivity is incorporated into the visual pigment rhodopsin (Hall, Bok & Bacharach 1968, 1969), supporting the hypothesis that the band of label observed by autoradiography corresponds to those disks whose rhodopsin molecules were synthesized in the presence of label. Continued membrane synthesis and disk formation results in the scleral displacement of previously-formed disks. Adult r.o.s. maintain a relatively constant length because the addition of new basal disks is balanced by the intermittent shedding of groups of old disks from r.o.s. tips. These disk packets are phagocytized by the adjacent pigment epithelium (p.e.), where they fuse with lysosomes and are digested (Young & Bok 1969; Bok & Young 1977). Autoradiograms of frog retinae first revealed that cone outer segments (c.o.s.) do not show a distinct band of radioactive material, but a diffuse labelling throughout (Young 1969). This difference in the renewal pattern of r.o.s. and c.o.s. has been correlated with a difference in topology of their membranes (Young 1969, 1970). It was originally believed that the absence of an accumulation of label into a band in c.o.s. indicated a lack of membrane synthesis in adult cones (Young 1969, 1970, 1971*a*) but more recent work has shown that mature mammalian cones probably renew their membranes (Hogan, Wood & Steinberg 1974; Anderson & Fisher 1975, 1976; Steinberg, Wood & Hogan 1977). A similar difference in the pattern of outer segment renewal has been observed in the rods and cones of all vertebrate species examined thus far, both in the adult and during development (Young 1967, 1970, 1971*a*, *b*; LaVail 1973; Godfrey 1974; Ditto 1975; Anderson & Fisher 1975, 1976; Besharse & Hollyfield 1976; Buyukmhici & Aguirre 1976; Fisher, Jacobs, Anderson & Silverman 1976).

The rate of r.o.s. renewal has been found to vary with the experimental temperature and lighting conditions in which the animals are kept (Young 1967), the kind of rod (in retinae containing both red and green rods) (Young & Droz 1968), the developmental stage (LaVail 1973; Besharse & Hollyfield 1976), and the species studied. It has been assumed that the rates of basal metabolism and r.o.s. renewal are related in a given species (Lolley & Schmidt 1974), because the difference in r.o.s. renewal time in the rat and frog parallels the difference in their basal metabolic rates.

We have studied the process of outer segment renewal in the photoreceptors of the adult and developing African clawed frog (*Xenopus laevis*), an anuran that is aquatic throughout its life history (Deuchar 1975). Although the developing visual system of *Xenopus* has been studied extensively (Gaze 1970; Jacobson 1970; Chung, Stirling & Gaze 1975; Hunt 1975; Jacobson 1976; Keating & Kennard 1976), there have been relatively few morphological descriptions of

Xenopus photoreceptors or p.e. either during development or in the adult (Denton & Pirenne 1952; Saxén 1954; Lanzavecchia 1960; Grillo & Rosenbluth 1972; Chung *et al.* 1975; Witkovsky *et al.* 1976).

In this paper we describe photoreceptor and p.e. morphology, and the process of outer segment renewal in the adult *Xenopus* retina. The two following papers present analogous observations during initial outer segment formation (Kinney & Fisher 1978*a*) and metamorphosis (Kinney & Fisher 1978*b*).

Materials and methods

(*a*) *Light microscopy and autoradiography*

Two small, adult male *Xenopus* (26 and 28 g) were injected in the dorsal lymph sac with 8 mCi of L-[4,5-^{3}H]leucine (sp.act. 51 Ci/mmol; 389 Ci/mg). The animals were kept at an average temperature of 22 °C under cyclic laboratory lighting conditions and were fed minced beef liver. Before sacrifice, animals were anaesthetized by immersion in 0.33 g/l tricaine methane sulfonate (MS-222) and their eyes were removed in the light at $3\frac{1}{2}$, $12\frac{1}{2}$, $18\frac{1}{2}$, and $24\frac{1}{2}$ days after injection. The lenses were removed and the eyes fixed for 12 h in 1.5 % glutaraldehyde in 0.067 M cacodylate buffer (pH 7.2) with 0.5 mg/ml calcium chloride. The tissue was refrigerated after 20 min of fixation and all subsequent solutions were refrigerated. It was then rinsed in three 20 min changes of isotonic buffer (0.067 M cacodylate, 0.5 mg/ml calcium chloride, and 55 mg/ml sucrose) and postfixed for $1\frac{1}{2}$ h in 2 % osmium tetroxide in veronal acetate buffer (pH 7.2) with 0.2 mg/ml calcium chloride. The tissue was rinsed in water and dehydrated in a graded ethanol–water series, transferred to propylene oxide, and embedded in araldite.

Sections of 0.5 μm were cut on a Porter-Blum MT-2B ultramicrotome until the area of the optic nerve head was reached. The sectioning angle was then adjusted to be parallel to the longitudinal axes of the outer segments. Some sections were stained with 1 % azure II–1 % methylene blue in 1 % sodium borate and observed by light microscopy (l.m.), while others were not stained but processed for autoradiography by dipping in Kodak Nuclear Track Emulsion (NTB2) diluted 1:1 with distilled water and maintained at 40 °C. The autoradiograms were kept in light-tight boxes at 4 °C for exposure times of 7 or 8 days and then processed in the dark at 16–17 °C by developing in Dektol for 2 min, washing briefly in 1 % acetic acid, and fixing in Kodak rapid fixer for 5 min. Following a water wash, the autoradiograms were stained with 1 % toluidine blue in 1 % sodium borate and observed by l.m.

Measurements were made with a calibrated graticule in a Zeiss Large Universal Research microscope on rods in the posterior retina which were at least 200 μm from the optic nerve head and whose entire outer segment length appeared within the plane of section. The distance between the centre of the band of label and the outer segment base was measured for twenty rods in each eye, measurement being

facilitated by the different staining properties of the inner and outer segments. The mean band displacement was calculated for each interval, and the method of least squares used to determine the average rate of band migration. The R^2 coefficient (given in figure captions) was calculated to determine the goodness of fit between the data points and the line defined by least squares. R.o.s. length and width were also measured, and their means calculated. R.o.s. renewal time was determined from the rate of band displacement and average r.o.s. length.

(*b*) *Electron microscopy*

An adult male *Xenopus* was anaesthetized and enucleated in the light. The lenses were removed to facilitate penetration of the fixative, and the eyes were fixed by immersion in cold 1.3 % osmium tetroxide buffered with veronal acetate (pH 7.2) and containing 15 mg/ml sucrose and 0.13 mg/ml calcium chloride. The tissue was dehydrated in a graded ethanol-water series, transferred to propylene oxide, and embedded in araldite.

Sections of 0.5 μm were cut until the optic nerve head was located, then a pyramid was made in a part of the posterior retina containing photoreceptors oriented parallel to the plane of section. Thin sections (600–800 Å)† of the pyramid were placed on bar grids, stained with uranyl acetate and lead citrate, and examined in a Siemens Elmiskop 1A electron microscope (e.m.).

Description of plate 1

Figures 1 and 2. Light micrographs of light-adapted *Xenopus* retina. Azure II-methylene blue.

Figure 1. All of the retinal layers are visible, from the ganglion cells (G) at the vitreal margin, to the photoreceptors (P) and pigment epithelium (p.e.) at the scleral border. Red blood cells are apparent in chloroidal capillaries bordering the p.e. Details of p.e. cytoplasm are largely obscured by pigment granules, except for two nuclei with prominent nucleoli. Photoreceptor outer segments stain darkly, their inner segments stain less darkly, and their nuclei stain lightly. (Magn. × 640.)

Figure 2. Long cylindrical outer segments of rods (R) clearly distinguish them from cones (C), which have short conical outer segments and a round oil droplet in their inner segments. Pigment granules occur in the apical p.e. cytoplasm but are not found in the fine p.e. processes (arrow) that extend between rod outer segments (r.o.s.). (Magn. × 1000.)

Figures 3–6. Light microscopic autoradiographs from posterior retinae of adult frogs injected with [^{3}H]leucine and serially sacrificed. Toluidine blue. (Magn. × 1200.)

Figure 3. Three and a half days after injection, a dense band of label is present near the base of each r.o.s. No such accumulation of label appears in cone outer segments (c.o.s.) (arrows and inset), which are diffusely labelled throughout their length. (Inset magn. × 1875.)

Figure 4. After 12½ days, the band of label has not changed in appearance but is located about half way along each r.o.s.

Figure 5. After 18½ days, the band of label in r.o.s. has been displaced further sclerally.

Figure 6. After 24½ days, the band of label has migrated to the tips of some r.o.s. and has disappeared from others. A phagosome displaying an obvious band of label (arrow and inset) is located in the p.e. above unlabelled rods. (Inset magn. × 1875.)

† 1Å = 0.1 nm = 10^{-10} m.

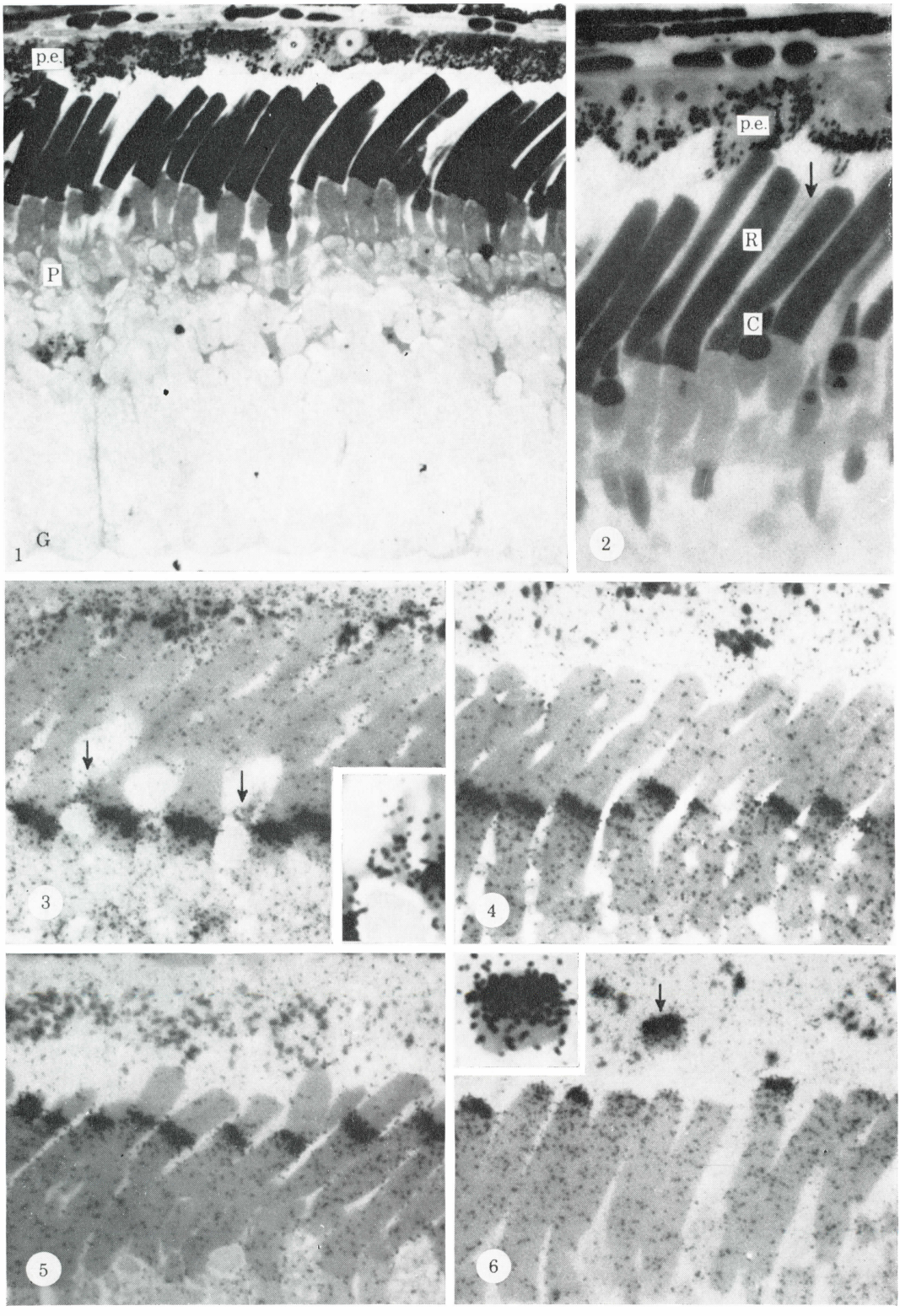

FIGURES 1–6. For description see opposite.

(*Facing p.* 134)

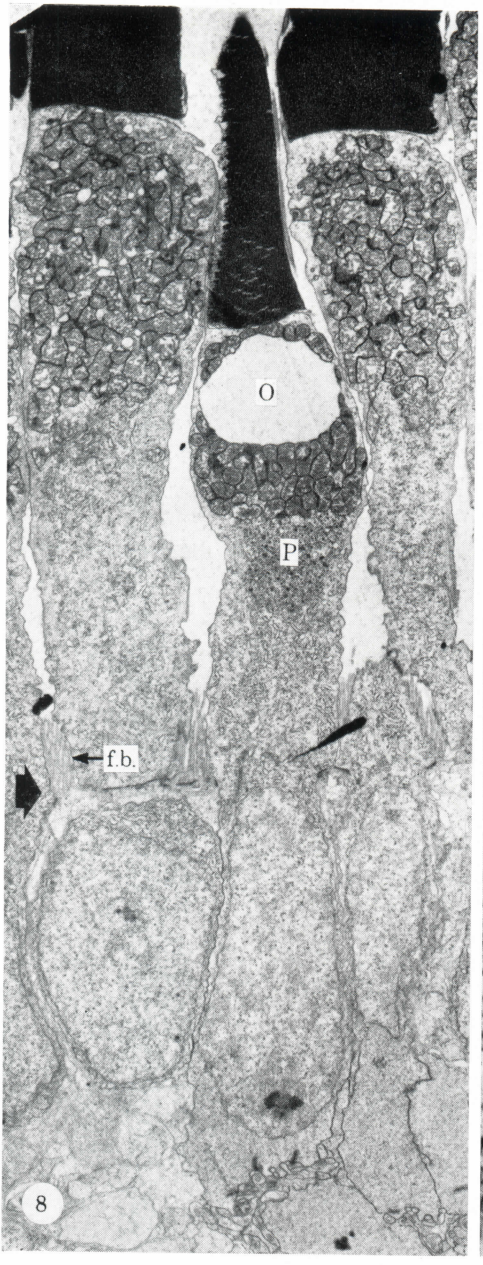

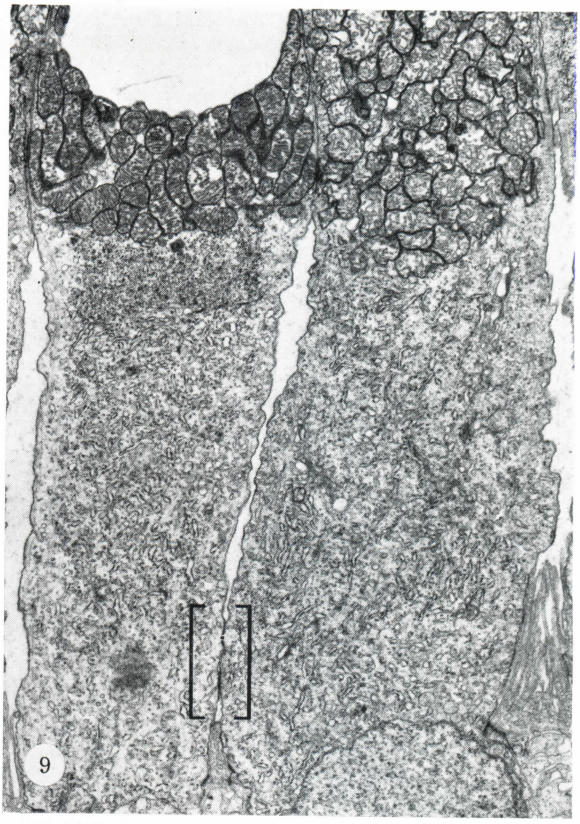

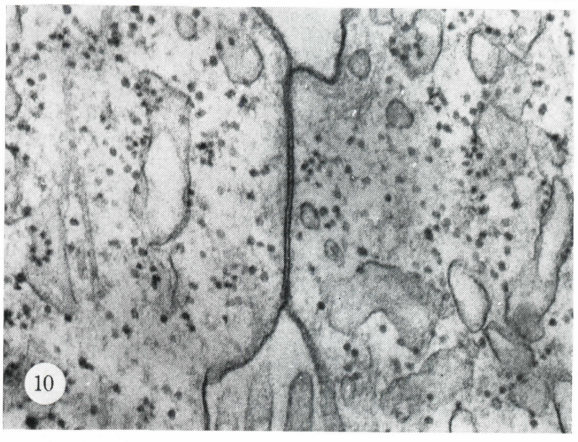

FIGURES 8–10. For description see opposite.

Results

(*a*) *Light microscopy and autoradiography*

The general morphology of the light-adapted *Xenopus* retina is illustrated by figure 1, plate 1. The retina is avascular, possessing choroidal circulation (at top of figure 1) and retinal vessels (not shown) which run along the vitreal surface. In figure 1, the nuclei of two p.e. cells are apparent but the epithelial cytoplasmic detail is obscured by numerous small pigment granules. The photoreceptors and p.e. are shown at higher magnification in figure 2, plate 1, where rods and cones are distinguishable from each other by both the size and shape of their outer segments, and the presence of a prominent, round oil droplet in each cone inner segment. The long, cylindrical r.o.s. extend to the apical border of the p.e., unlike the much shorter, tapered c.o.s. Thin apical processes of the p.e. which extend between the r.o.s., towards the c.o.s. tips, do not contain pigment granules.

Autoradiographs from eyes removed at different times after the injection of [^{3}H]leucine (figures 3–6, plate 1) demonstrate the distribution of radioactive protein in the photoreceptors. Three and a half days after injection (figure 3) a distinct band of radioactive material appears near the base of each r.o.s. The cone in the centre of figure 3, displayed at higher magnification in the inset, shows the typical pattern of diffuse labelling found in all c.o.s. in this study. After $12\frac{1}{2}$ days the band of label is located half way up each r.o.s. (figure 4), after $18\frac{1}{2}$ days it is approaching the r.o.s. tips (figure 5), and by $24\frac{1}{2}$ days (figure 6) it is located at the tips of several r.o.s. and also appears, for the first time, in labelled phagosomes in the p.e. (inset, figure 6).

On the basis of l.m. morphology and autoradiography, only one kind of rod and cone was observed in the *Xenopus* retina. All r.o.s. are approximately the same size, their bases are located at the same level, and their bands of label are displaced at the same rate. In a freshly-dissected, dark-adapted retina, red-coloured rods but no green-coloured rods were found (Kinney 1977). No obvious morphological or autoradiographic differences were found between cones.

Description of plate 2

Figures 8–10. Electron micrographs of photoreceptors.

Figure 8. The inner segment of a cone is readily distinguished from that of adjacent rods by the presence of both an oil droplet (O) among the mitochondria of the ellipsoid, and a paraboloid (P). Rod and cone myoids, nuclei, and synaptic terminals are similar morphologically. Müller cell processes generally isolate adjacent receptors below the level of the outer limiting membrane (arrow), and terminate sclerally in the fine villous processes of the fibre basket (f.b.). P.e. cell processes do not extend sclerally to the inner segments. (Magn. × 3900.)

Figure 9. Area of close membrane apposition (brackets) between a rod and cone inner segment just sclerad to the fibre basket. (Magn. × 5850.)

Figure 10. Higher magnification micrograph of a contact between receptor inner segments; plasma membranes of adjacent cells appear particularly dense and parallel at these contacts. (Magn. × 50000.)

The mean and range of the measurements of band displacement and r.o.s. length for each labelling period are displayed graphically in figure 7, from which it is apparent that band displacement with time is linear and the length of r.o.s. relatively constant. Mean r.o.s. length (dashed line in figure 7) and width are 45 and 8 μm, respectively. A straight line (continuous line in figure 7) generated by the method of least squares fits the band displacement data very well. Because both r.o.s. width and disk spacing vary negligibly, the constant rate of band

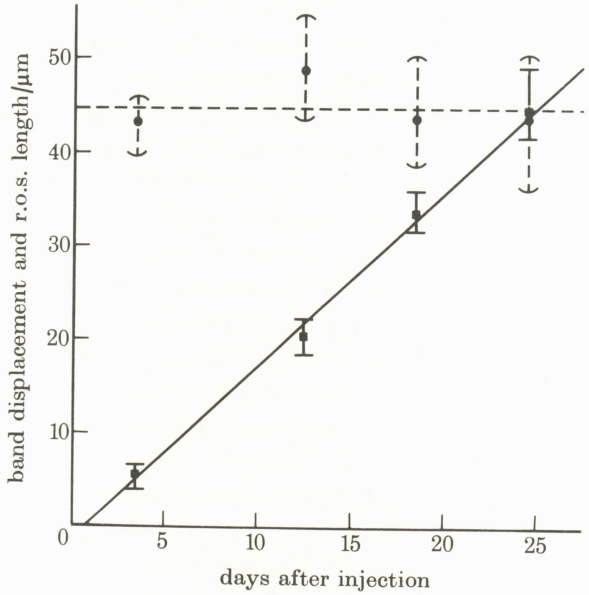

FIGURE 7. R.o.s. renewal in adult *Xenopus*. The mean distance of band displacement (■) and r.o.s. length (●) are plotted as a function of days after labelling. Ranges of these values are indicated by brackets. Average r.o.s. length (dashed line) is 44.8 μm. A straight line (continuous) fitted to the band displacement data by the method of least squares, yields a band migration rate of 1.86 μm/day (R^2 = 99 %). R.o.s. renewal time (24 days) can be approximated from the time at which the two lines in the graph intersect or by dividing the average r.o.s. length by the average rate of band displacement.

migration indicates a constant rate of r.o.s. membrane (and thus disk) addition at 1.86 μm/day (equivalent to 78 disks/day). A r.o.s. renewal time of 24 days is calculated from r.o.s. length and band displacement rate, and can also be derived from figure 7 as the time at which the two lines intersect. The ranges of r.o.s. length and band displacement measurements first overlap at $24\frac{1}{2}$ days after injection, corresponding to the first time at which labelled phagosomes were observed. The relative constancy of adult r.o.s. length indicates that the overall addition of new membrane at the base is balanced by an equal loss of membrane at the r.o.s. tip, occurring by the discontinuous process of disk shedding and phagocytosis at an average rate of 1.86 μm/day.

(*b*) *Electron microscopy*

Electron microscopy demonstrates additional morphological distinctions between kinds of photoreceptors in *Xenopus*. Figure 8, plate 2, illustrates such differences in rod and cone inner segments. All cone inner segments observed possess a prominent, round oil droplet surrounded by mitochondria, vitread to which is the paraboloid, an accumulation of glycogen granules. In contrast, adult rod inner segments lack both oil droplets and paraboloids. The remaining myoid region, nucleus, and synaptic terminals of rods and cones are structurally similar. Autophagic vacuoles were occasionally observed in receptor inner segments. Photoreceptor nuclei occupy a single retinal layer.

Vitread to the outer limiting membrane (o.l.m.), adjacent photoreceptors are generally separated by Müller cell processes except near the synaptic terminals. Sclerad to the o.l.m., Müller cells terminate as fine processes forming the fibre basket (Dowling & Sidman 1962), above which photoreceptor inner segments are only separated by the extracellular matrix. Fine radial processes or fins were occasionally seen projecting from photoreceptor inner segments in the area of the fibre basket. Sclerad to the fibre basket, specialized contacts were occasionally observed between adjacent rods and cones (figures 9, 10, plate 2). These contacts appear as the particularly dense and parallel membranes characteristic of gap junctions in tissue not stained *en bloc* with uranyl acetate (Brightman & Reese 1969).

By ultrastructural criteria, only one kind of rod was found in *Xenopus*, confirming our histological and autoradiographic observations. Except at the r.o.s. base (where the invaginating membranes retain continuity with the plasma membrane) the rod disks are separated from the outer cell membrane, their edges having a rounded, button-like structure (left inset, figure 11, plate 3). When sectioned obliquely, r.o.s. appear lobulated or scalloped, with some 15 to 20 scallops per cell arranged in register. Thin calycal processes from the inner segment extend part way up the r.o.s. and lie in the indentations between scallops. In longitudinal sections the r.o.s. scallops appear as occasional longitudinal striations (as in the central r.o.s. of figure 11) which correspond to areas of discontinuity in the disk membranes at the cleft between two scallops. Except for such discontinuities, r.o.s. disk membranes have a very regular structure, with a disk spacing of 42 disks/μm. C.o.s. are also composed of a stack of membranes oriented perpendicular to the long axis of the cell. Longitudinal sections of c.o.s. demonstrate that they lack an external plasma membrane (right inset of figure 11), except in areas near the connecting cilium, such that an entire c.o.s. consists of infoldings of the external plasma membrane. *Xenopus* c.o.s. and r.o.s. also differ in that the former did not show the internal discontinuities characteristic of scalloped outer segments. By our fixation, membrane spacing in c.o.s. (42 'disks'/μm) is similar to r.o.s., but the extracellular space in cones is narrower than the rod intra-disk space. Additionally, c.o.s. membranes exhibit somewhat regularly-spaced dilations of the extra-

cellular space which are displaced from each other both laterally and vertically. No convincing ultrastructural evidence was found for the existence of more than one kind of cone in *Xenopus*.

The apical border of the p.e. contacts the tips of r.o.s., and numerous fine p.e. cell processes extend vitreally between the r.o.s., some as far as the tips of the c.o.s. (as in figure 11). These processes appear largely devoid of organelles, but do contain small vesicles and microfilaments which originate within the apical p.e. cytoplasm. Although present in the apical p.e. cytoplasm of this light-adapted retina, pigment granules were never observed within these processes. Occasionally, inclusions were observed within p.e. cell processes, located directly above blunt-tipped c.o.s. yet below the level of the tips of adjacent r.o.s., whose membranes displayed the ultrastructural features of c.o.s. membranes (see figure 11).

The p.e. (figures 12, 13, plate 4) is bordered sclerally by Bruch's membrane separating it from the choroidal capillaries. The basal border of the p.e. is largely flat, except for occasional infoldings of plasma membrane near the lateral border of adjacent cells. The basal cytoplasm contains numerous mitochondria and the cell nucleus, whereas the many small pigment granules are largely confined to the apical cytoplasm (figure 12). Smooth endoplasmic reticulum is abundant throughout most of the cell but sparse near the basal border. Numerous ribosomes, a few Golgi bodies, small oil droplets, primary lysosomes, and residual bodies (possessing areas of high electron density) are scattered throughout the cell. Several myeloid bodies occur in close association with the nuclear membrane (figure 12) while others do not. Junctional complexes between adjacent cells occur about 1 μm from the apical border.

Whereas groups of disks actually in the process of detaching from r.o.s. tips

---

Description of plate 3

Figure 11. Photoreceptor outer segments and the adjacent p.e. Tips of the r.o.s. are in close proximity to the apical border of the p.e., and many fine p.e. processes (containing microfilaments: open arrow) extend to the level of the tips of c.o.s. (dark arrows). R.o.s. disks are scalloped, as evidenced by the longitudinal striations (see central r.o.s.) corresponding to clefts between scallops. A calycal process occurs at the base of the rightmost r.o.s. At the edge of r.o.s. (left inset) the membranous disks are separated from the enclosing plasma membrane, except at the r.o.s. base. By contrast, the membranes of c.o.s. retain continuity with one another at their perimeter (right inset), and are not bounded by a separate cell membrane. Note packet of outer segments membranes (large dark arrow) in a p.e. process above c.o.s. (Magn. × 6000. Insets magn. × 60000.)

Description of plate 4

Figures 12 and 13. Surveys of p.e. demonstrating the loose layering of organelles between the basal (top of picture) and apical (bottom of picture) cell borders. Note Bruch's membrane (B), infoldings of the basal plasma membrane at the border between adjacent cells (open arrow), and junctional complexes near apical borders (dark arrows). Cytoplasmic organelles include mitochondria, myeloid bodies (M), Golgi bodies (G), lipid droplets (L), pigment granules (g), smooth endoplasmic reticulum (s.e.r.), primary lysosomes (p), large phagosomes (P), and residual bodies (R). (Magn. × 6000.)

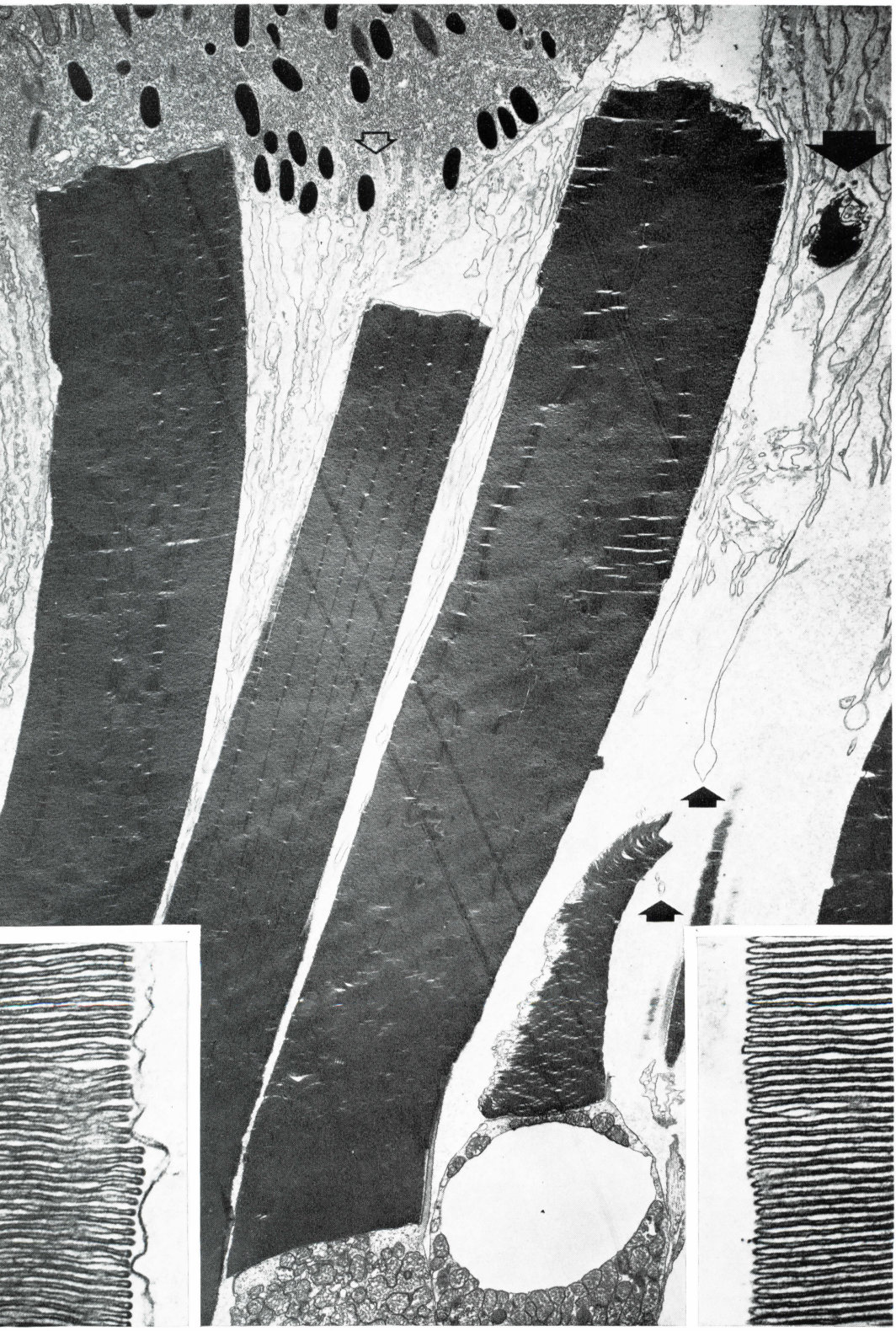

FIGURE 11. For description see opposite.

(*Facing p.* 138)

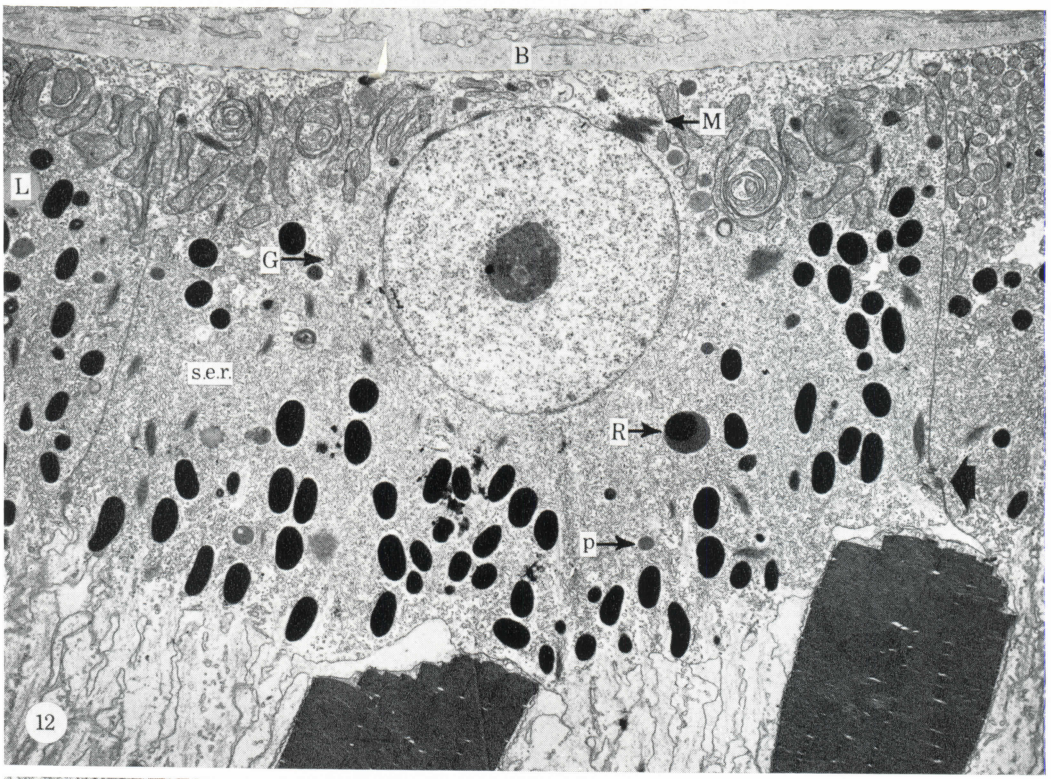

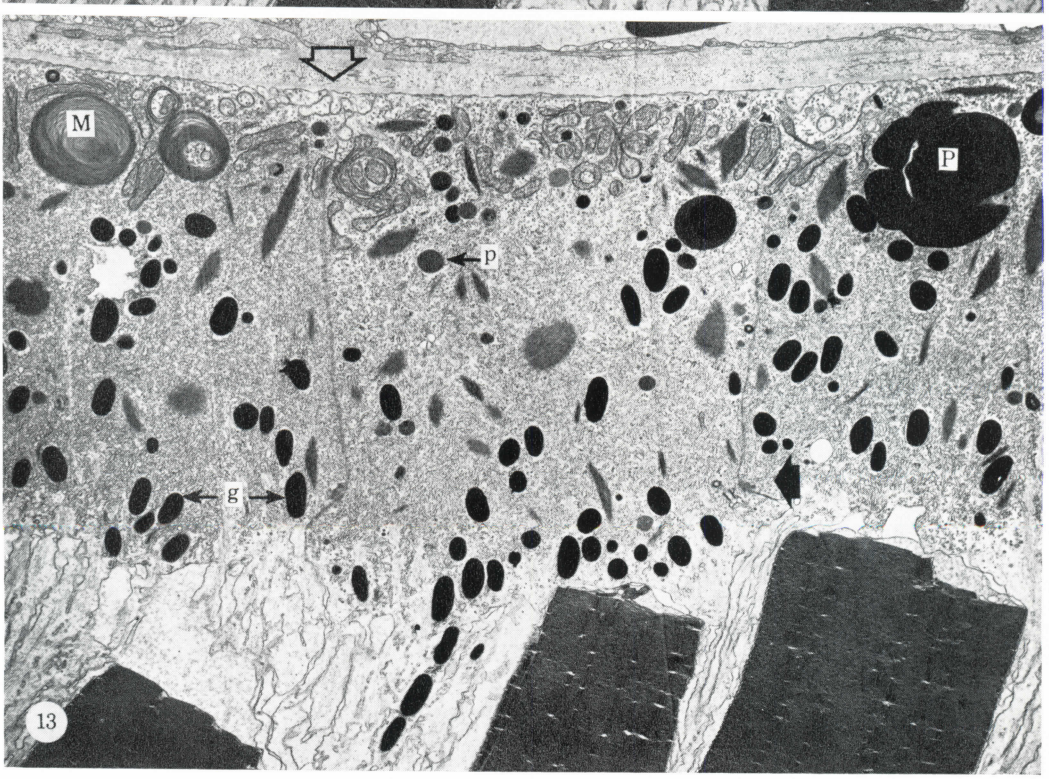

FIGURES 12 AND 13. For description see p. 138.

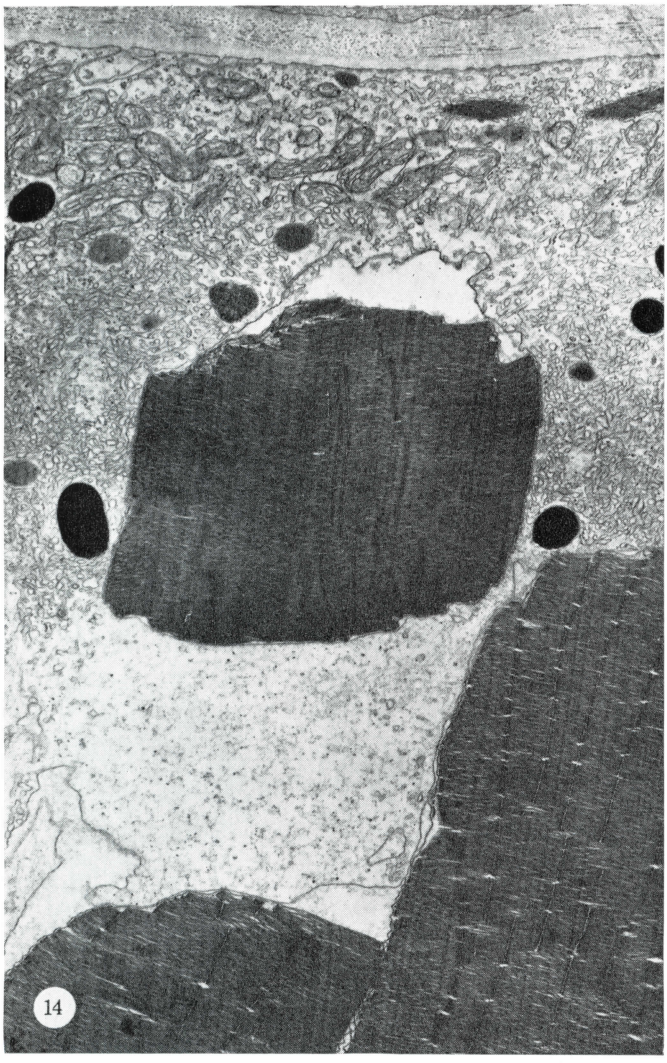

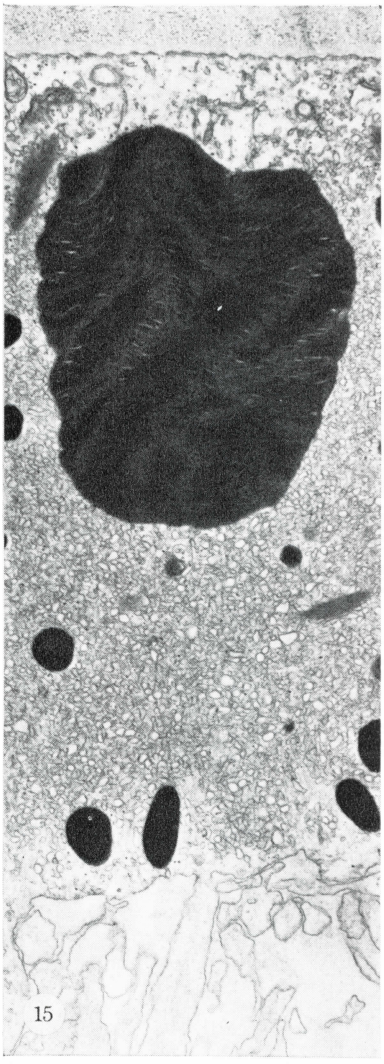

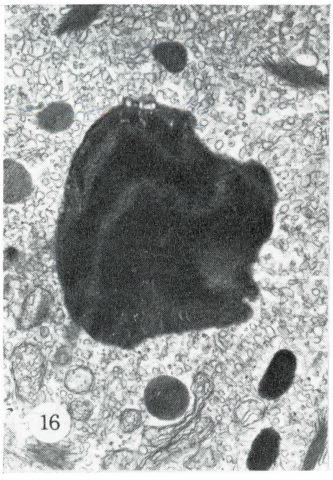

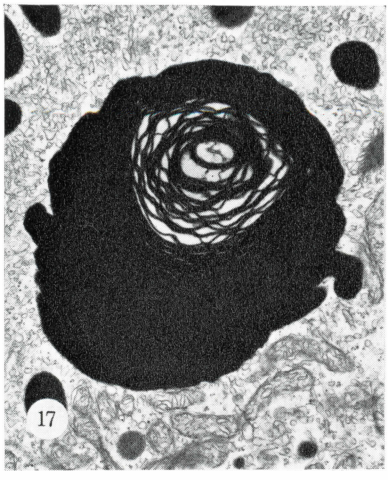

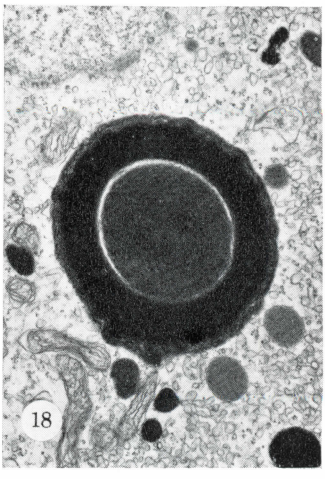

FIGURES 14–18. For description see p. 139.

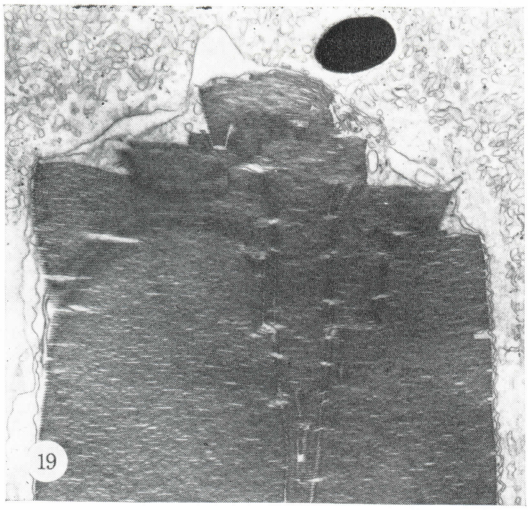

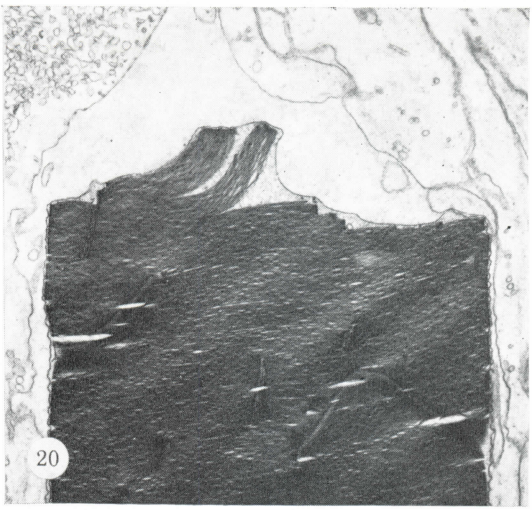

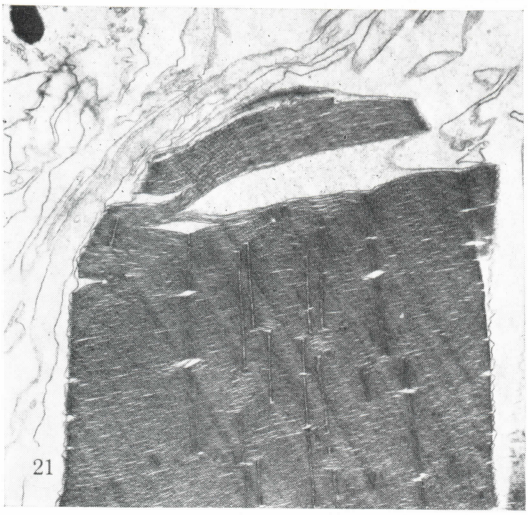

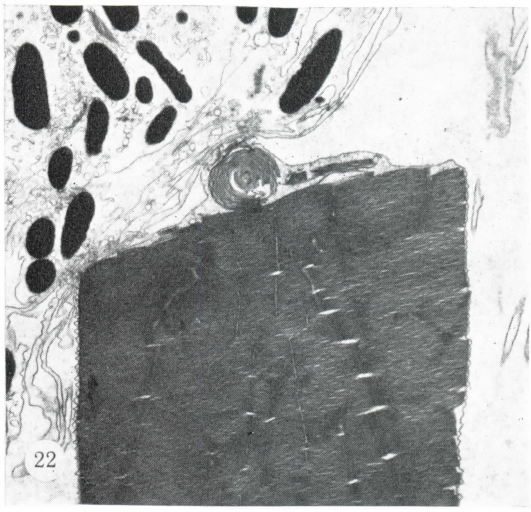

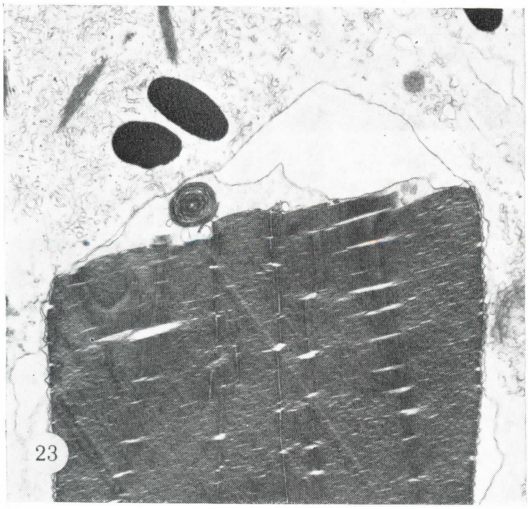

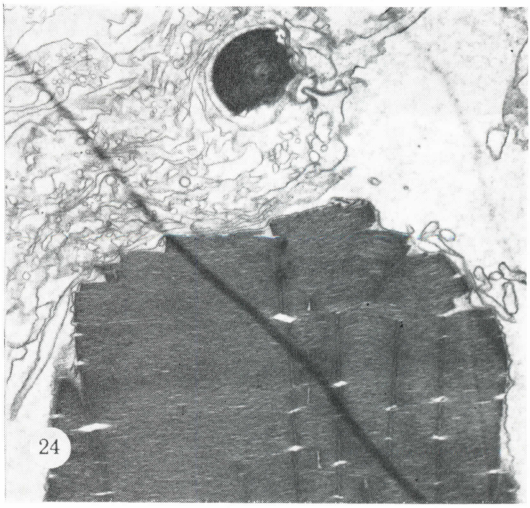

FIGURES 19–24. For description see opposite.

are seldom observed, examples of large phagosomes in various stages of digestion in the p.e. are found quite readily (figures 14–18, plate 5). Evidently the phagosome in figure 14 has recently been shed from the underlying r.o.s., because its membranes appear intact and the cytoplasm below it contains few organelles. This phagosome is 4.5 μm high, representing the number of disks synthesized by a rod during about 2½ days. The phagosome in figure 15 is apparently of earlier origin, in that it is farther from the apical border and its membranes are distorted and display areas of high electron density where individual membranes are no longer discernible. Based on the criteria of increasing distortion and membrane density, the phagosomes illustrated in figures 16–18 are progressively more digested. Another phagosome representing yet a later stage in the digestion of rod disk membranes appear in figure 13, plate 4.

The tips of some r.o.s. are noticeably uneven or tiered, consisting of several steps whose vertical edges appear to coincide with the membrane discontinuities corresponding to clefts between scallops in the disks below (figures 11, 12, 13, 19, 20, 24, plates 3, 4 and 6). Small packets of partial disk membranes (figures 20, 21, plate 6) and small circular whorls of membrane (figures 22, 23, plate 6) appear to be detaching from other r.o.s. tips. Phagosomes similar in size to these whorls and much smaller than the width of a *Xenopus* rod are sometimes found within the p.e. processes above rod tips (figure 24, plate 6).

Description of plate 5

Figures 14–18. Examples of several successive stages in the digestion of large rod phagosomes by the p.e. (see text for description). (Magn. × 9000.)

Description of plate 6

Figures 19–24. Possible sequences of stages in the shedding and phagocytosis of small phagosomes from r.o.s. tips. Note membrane discontinuities in the disks of the outer segments indicative of the presence of clefts in these planes of section.

Figure 19. A r.o.s. tip which consists of several obvious tiers or steps. (Magn. × 12000.)

Figure 20. Two small groups of partial disks (which had probably formed a tier) are curling away from the membranes below them. (Magn. × 18000.)

Figure 21. A small packet of disks narrower than the entire r.o.s. is apparently detaching from its tip; the right hand edge of this packet coincides with a striation in the outer segment below it. (Magn. × 10000.)

Figure 22. A small packet of membranes curling up to form a circular whorl; one end of the whorl is aligned with clefts in the discs below it, with which it retains minimal contact. (Magn. × 8000.)

Figure 23. In another r.o.s. tip a whorl of concentric membranes has detached from the remaining outer segment disks but is still within the r.o.s. cytoplasm. The length of the membrane pieces forming this whorl is similar to the distance between clefts in the underlying disks. (Magn. × 9000.)

Figure 24. A small phagosome appears within a p.e. process directly above the tip of a r.o.s. The length of the longest piece of membrane visible in this inclusion is about 1.3 μm, which is much less than the width of an entire r.o.s. but similar to the distance between clefts in the r.o.s. below it. (Magn. × 10000.)

Discussion

(*a*) *Autoradiography*

The pattern of labelling we have observed in the photoreceptors of adult *Xenopus* following the injection of [^{3}H]amino acid is typical of that described in all other vertebrate retinae examined to date (rat, mouse, frog: Young 1967; monkey; Young 1971*b*; chick: Godfrey 1974; salamander: Ditto 1975; diurnal squirrels: Anderson & Fisher 1975, 1976, Fisher *et al.* 1976; dog: Buyukmhici & Aguirre 1976; cave salamander: Besharse & Hollyfield 1976). A distinct band of label present soon after injection at the base of the r.o.s. becomes displaced sclerally with time; label never accumulates as a band in c.o.s. Since radioactive protein visualized by autoradiography as a band of label in *Rana* r.o.s. has been shown to be mainly the visual pigment rhodopsin (Hall *et al.* 1968, 1969), and since the visual pigment in *Xenopus* rods is porphyropsin (Bridges, Hollyfield, Witkovsky & Gallin 1977) [in which opsin is combined with dehydroretinal (vitamin A_2) instead of retinal (vitamin A_1); Bridges 1972], it is likely that the band of label in *Xenopus* r.o.s. consists mainly of radioactive porphyropsin. We found no autoradiographic evidence for the presence of more than one kind of rod in *Xenopus*, in that the band of label migrated in parallel in all r.o.s., whereas in *Rana* the rate of band displacement is faster in red than green rods (Young & Droz 1968).

The rate of disk displacement within r.o.s. was constant under the conditions of our experiment: a relatively constant temperature and a daily light/dark cycle. The rate of r.o.s. renewal found in *Xenopus* (78 disks/day) is more than twice that reported for red rods in *Rana esculenta* (36 disks/day) (Young & Droz 1968) – a surprising difference in as much as *Xenopus* and *Rana* have similar metabolic rates (Altman & Dittmer 1974) and previous studies suggested that r.o.s. renewal rate and basal metabolic rate are directly related (Lolley & Schmidt 1974). Moreover, even though experimental temperature and lighting conditions can affect renewal rate (Young 1967), it is unlikely that these factors account for this two-fold difference, especially since the *Xenopus* in the present study and the *Rana* reported in experiments by Young & Droz (1968) were kept under essentially the same conditions of temperature and illumination.

All previous reports on r.o.s. renewal rates are for species having rhodopsin photopigments. The *Xenopus* rod pigment is porphyropsin, and because rhodopsins are reportedly more stable than their homologous porphyropsins (Bridges 1972), this difference may have favoured the evolution of a higher renewal rate for rods containing porphyropsin. R.o.s. renewal rate was therefore measured in the goldfish (*Carassius auratus*) (another freshwater cold-blooded vertebrate with porphyropsin-containing rods; Marks 1965), and found to be 0.59 μm/day (renewal time of 58 days) in fish kept in the same conditions as *Xenopus* (Kinney 1977). Although the metabolic rates of these two species are not directly comparable because they belong to different vertebrate classes, the finding that renewal

TABLE 1. RATE OF ROD OUTER SEGMENT (r.o.s.) RENEWAL IN DIFFERENT VERTEBRATES

animal (source(s) for data)	r.o.s. dimensions: length (μm)	diameter (μm)	volume† (μm³)	measures of renewal rate: renewal time (day)	distance per day (μm/day)	volume per day (μm³/day)
monkey (*Macaca mulatta*) (Young 1971*b*)	28.4	1.5	50	12.8	2.22	3.9
dog (Hebel 1971; Buyukmhici & Aguirre 1976)	12	1	9.5	5	2.4	1.9
mouse (LaVail 1973)	22.2	1.5	40	10.4	2.13	3.85
rat (LaVail 1976)	25	1.5	44	10	2.5	4.4
tree squirrel (*Sciurus carolinensis*) (Anderson & Fisher 1976)	12	2	38	5	2.4	7.6
Rana pipiens and *esculenta* (Young 1967; Liebman & Entine 1968)	50	6	1422	45	1.1	32
Xenopus laevis	45	8	2275	24	1.86	95
goldfish (*Carassius auratus*) (Stell & Harosi 1976; Kinney 1977)	35	2	110	58	0.6	1.9
cave salamander (*Typhlotriton spelaeus*) (Besharse & Hollyfield 1976)	15	3.7	160	43	0.35	3.7

† R.o.s. volume calculated as that of a cylinder from data on length (L) and diameter (D): volume = $\frac{1}{4}\pi D^2 L$.

is much slower in the goldfish than in *Xenopus* suggests that the difference in renewal rates of *Rana* and *Xenopus* is unrelated to the difference in their photopigments.

Because of the disparity in r.o.s. width between species, the most physiologically appropriate measure of renewal rate may not be disks/day, μm/day, or renewal time, but surface area of membrane renewed per day, i.e. μm²/day. Assuming a constant number of visual pigment molecules per unit of membrane surface area, such a measure would correspond to the rate of renewal of visual pigment molecules. Because disk spacing (Gras & Worthington 1969; Dunn 1973; Montal & Korenbrot 1977) and visual pigment density (Harosi 1975) in different vertebrate species are quite similar, a convenient estimate of r.o.s. disk membrane surface area can be obtained by calculating the r.o.s. volume as a cylinder. Table 1 presents the rates of r.o.s. renewal reported for different species, expressed as renewal time, μm renewed per day, and volume or μm³ renewed per day. Although the mammals have a shorter renewal time and higher renewal rate when expressed as μm/day than the cold-blooded species, a comparison of renewal rates in *Xenopus* and *Rana* shows that these measures of r.o.s. renewal rate do not always

correlate with metabolic rate. When renewal is expressed as volume of outer segment material replaced per day, even greater disparities are found between renewal and metabolic rates, in that by this measure renewal is considerably faster in both species of frog than in the mammals. These comparisons must be regarded as somewhat conditional because they are based on data from a number of sources collected under different experimental conditions; nevertheless, they do fail to reveal any general correlation between any measure of r.o.s. renewal rate and basal metabolism. Photoreceptor packing density and the number of receptors per p.e. cell vary with species, and it is possible that r.o.s. renewal rate is affected by such factors, reflecting a limited phagocytic capacity of the p.e.

(*b*) *L.m. and e.m. morphology*

(i) *Photoreceptors*

Although the literature includes contradictory findings (e.g., one report of green rods in *Xenopus*; Denton & Pirenne 1952), the best conclusion from previous morphological (Denton & Pirenne 1952, 1954; Saxén 1954; Lanzavecchia 1960; Hailman 1976), visual sensitivity (Hogben & Slome 1936; Hogben 1942; Burgers 1952; Denton & Pirenne 1952, 1954; Silver née Strange 1963; Cronly-Dillon & Muntz 1965; Muntz 1967), and photopigment (Bridges *et al.* 1977) studies is that the *Xenopus* retina has one kind of porphyropsin-containing red rod and one or two kinds of cones. Studies of visual behaviour in *Xenopus* show that this frog is primarily nocturnal (Stewart 1967) and photophobic (Denton & Pirenne 1951, 1954), with poor (if any) colour vision (Burgers 1952).

Our morphological and autoradiographic observations in the *Xenopus* retina provide evidence for a single kind of rod which corresponds to the red rods of other amphibians [amphibian green rods can be distinguished from the more common red rods on the basis of visual pigments (Liebman & Entine 1968), morphology (Nilsson 1964), and outer segment renewal rate (Young & Droz 1968)]. Our failure to observe green rods in *Xenopus* agrees with other data on *Xenopus* photopigments (Bridges *et al.* 1977), visual cell morphology (Saxén 1954; Lanzavecchia 1960; Hailman 1976), and visual sensitivity (Muntz 1967).

Although only one kind of cone was observed in this study, the argument for a single kind of cone in *Xenopus* is harder to establish inasmuch as visual sensitivity studies have not ruled out the possibility of two kinds (Muntz 1967), cone pigments are not readily extracted (Rodieck 1973), and the fact that cones containing different visual pigments may not differ morphologically (Stell & Harosi 1976). Though Hailman (1976) reported the presence of double cones in unfixed, unsectioned *Xenopus* retinae examined by l.m., they were not found in this study nor in studies by Saxén (1954) or Lanzavecchia (1960).

With the advent of electron microscopy, Lanzavecchia (1960) characterized more details of photoreceptor structure in *Xenopus* than had been described previously, including ultrastructural features of outer segment membranes that are typical of amphibian receptors (Nilsson 1965) and similar to those described

here. However, Lanzavecchia did not report the presence of cone paraboloids, which were found consistently in cones in this study and he reported that *Xenopus* rods, as well as cones, have an oil droplet in the inner segment. We observed oil droplets in larval rods, but these disappeared well before adulthood (Kinney & Fisher 1978*a*).

Saxén (1954) compared the morphology of the *Xenopus* and *Rana* retinae and found them to be similar in many respects but not identical. A comparison of the fine structure of *Xenopus* and *Rana* (Nilsson 1964, 1965) retinae reveals that *Xenopus* rods and *Rana* red rods are similar, as is the relation between Müller cell processes and receptors. Moreover, *Xenopus* cones resemble single cones in *Rana* except that the former contain paraboloids. P.e. processes in *Rana* are longer, often extending sclerally to overlap the Müller cell processes near the o.l.m. whereas in *Xenopus* they do not extend past the outer segments. The lateral fins and inter-receptor (presumed gap) junctions that we have observed just sclerad to the o.l.m. have not been described in *Rana*, where it appears that p.e. cell processes isolate many adjacent receptors. At the level of the o.l.m., gap junctions between neighbouring photoreceptors have been reported only in retinae of the axolotl (Custer 1973) and toad (Fain, Gold & Dowling 1976). In the latter study electrical coupling, presumably mediated by these junctions, was demonstrated between red rods.

(ii) *Pigment epithelium*

The retinal p.e. of *Xenopus* is, with a few exceptions, morphologically similar to that of *Rana* (Porter & Yamada 1960; Nilsson 1964). Whereas in *Xenopus* the junctional complexes between adjacent cells are located near the apical border, in *Rana* (Porter & Yamada 1960) they are nearer the basal border. The myeloid bodies and oil droplets observed in the *Xenopus* p.e. appear to be smaller and fewer in number than in *Rana*. Hailman (1976) found no oil droplets in the p.e. of *Xenopus*, but his observations were limited to l.m examination of unfixed, unsectioned tissue. In the p.e. we found inclusions which appear to represent various stages in the digestion of phagosomes, as well as primary lysosomes and residual bodies. P.e. processes in *Xenopus* contain microfilaments similar to those recently described in the *Rana* p.e. (Murray & Dubin 1975). The *Xenopus* p.e. does not exhibit photomechanical pigment granule migration (Saxén 1954), thus the presence of microfilaments in *Xenopus* p.e. processes suggests that these filaments serve other functions. This same conclusion has been made for the monkey retina, where it was suggested that microfilaments may stabilize the p.e. processes mechanically and/or function in the phagocytosis of shed outer segment disks (Burnside & Laties 1976). Yamada (1969) suggested that myeloid bodies function as photosensory organelles for pigment migration, but in *Xenopus* myeloid bodies obviously cannot perform this function.

(iii) *Shedding and phagocytosis of outer segments*

Our ultrastructural observations indicate that the shedding and subsequent phagocytosis of large packets of rod disks as first described in *Rana* (Young & Bok 1969) occurs similarly in *Xenopus*. Only infrequently did we find large groups of disks in the actual process of detaching from r.o.s. tips. Recent studies have demonstrated a burst of disk shedding following the onset of light in rats (LaVail 1976), *Rana* tadpoles (Hollyfield, Besharse & Rayborn 1976) and adults (Basinger, Hoffman & Matthes 1976) kept on a cyclic lighting schedule; a similar phenomenon occurs in *Xenopus* (Besharse, Hollyfield & Rayborn 1977). If retinal specimens are not fixed at the appropriate time, and if the detachment process itself is rapid, we would expect to rarely find disks in the actual process of shedding.

In *Xenopus*, as in *Rana* (Hollyfield *et al.* 1976), two different kinds of membrane packets can be shed from rods, one corresponding to the large phagosomes originally described by Young & Bok (1969) and illustrated in figures 14 and 15, plate 5, and the other corresponding to a second population of considerably smaller phagosomes (see figure 24, plate 6). Hollyfield *et al.* (1976) recently described a population of 'small' phagosomes (1–2 μm in diameter) in the p.e. of *Rana* tadpoles, the relative number of which remained constant throughout the light/dark cycle (unlike the number of large phagosomes which increased after the onset of light). The present study has revealed similar small phagosomes in the *Xenopus* p.e., as well as rod tips from which such structures appeared to be detaching. The relative ease with which we observed the detachment and phagocytosis of small phagosomes supports the conclusion of Hollyfield *et al.* (1976) that they are not shed cyclically.

A morphological basis for the origin of such small phagosomes is suggested on the basis of these observations: they may represent small stacks of *partial* disk membranes shed from one or more individual r.o.s. scallops. This suggestion is supported by our observation of several possible stages in the detachment of such structures, as illustrated by figures 19–23, plate 6. The edges of these detaching membranes appear to coincide with membrane discontinuities representing clefts between r.o.s. scallops; such discontinuities are commonly evident in the planes of section containing detaching partial disks and small phagosomes, in both our study and that of Hollyfield *et al.* (see their figs 14–17). Furthermore, these small phagosomes are similar in size to r.o.s. scallops and considerably smaller than entire r.o.s. disks in these retinas. Vertebrate r.o.s. are commonly scalloped, the depth of the clefts (Rodieck 1973) and number of scallops per disk varying between different animals, the latter increasing with increasing rod diameter (Steinberg & Wood 1975). Thus shedding of small phagosomes may be related to a mechanical instability at the tips of r.o.s. which have a large diameter coupled with numerous deep clefts (as in amphibian retinae). This phenomenon may be found to occur in other species whose r.o.s. have multiple deep clefts.

Cone shedding and phagocytosis have been documented in human (Hogan

et al. 1974; Steinberg *et al.* 1977) and diurnal squirrel (Anderson & Fisher 1975, 1976) retinae, but not in any non-mammalian retina. Although we have no conclusive evidence for cone-shedding in *Xenopus*, our observation of phagosomes with an internal structure reminiscent of c.o.s. membranes and located within p.e. processes below the level of r.o.s. tips (as in figure 11, plate 3) makes it tempting to speculate that this process occurs in *Xenopus*.

The authors wish to thank Mr R. Gill for his technical assistance, Dr J. F. Case, Dr. G. H. Jacobs, and Dr R. H. Steinberg for their critical comments on the manuscript. The work was supported by a U.S. Public Health Service N.I.H. grant no. EY00888 to S.K.F. Work contained in this paper was submitted to the University of California by M.S.K. as partial fulfilment of the requirements for the Ph.D. degree.

References

Altman, P. L. & Dittmer, D. S. 1974 *Biology data book*, vol. 3. Bethesda: Fedn Am. Socs exp. Biol.

Anderson, D. H. & Fisher, S. K. 1975 Disc shedding in rodlike and conelike photoreceptors of tree squirrels. *Science, N.Y.* **187**, 953–955.

Anderson, D. H. & Fisher, S. K. 1976 The photoreceptors of diurnal squirrels: outer segment structure, disc shedding, and protein renewal. *J. ultrastruct. Res.* **55**, 119–141.

Basinger, S., Hoffman, R. & Matthes, M. 1976 Photoreceptor shedding is initiated by light in the frog retina. *Science, N.Y.* **194**, 1074–1076.

Besharse, J. C. & Hollyfield, J. G. 1976 Renewal of normal and degenerating photoreceptor outer segments in the ozark cave salamander. *J. exp. Zool.* **198**, 287–302.

Besharse, J. C., Hollyfield, J. G. & Rayborn, M. 1977 Turnover of rod photoreceptor outer segments: membrane addition and loss in relationship to light. *J. Cell Biol.* **75**, 507–527.

Bok, D. & Young, R. W. 1977 Phagocytic properties of the retinal pigment epithelium. In *The retinal pigment epithelium* (eds K. M. Zimm & M. F. Marmor). Boston: Harvard University Press. (In the press.)

Bridges, C. D. B. 1972 The rhodopsin-porphyropsin visual system. In *Handbook of sensory physiology: Photochemistry of vision* (ed. H. J. A. Dartnall), vol. VII/1, pp. 417–480. Berlin: Springer-Verlag.

Bridges, C. D. B., Hollyfield, J. G., Witkovsky, P. & Gallin, E. 1977 The visual pigment and vitamin A of *Xenopus laevis* embryos, larvae and adults. *Expl Eye Res.* **24**, 7–13.

Brightman, M. W. & Reese, T. S. 1969 Junctions between intimately apposed cell membranes in the vertebrate brain. *J. Cell Biol.* **49**, 648–677.

Burgers, A. C. J. 1952 Optomoter reactions of *Xenopus laevis*. *Physiologia comp. Oecol.* **2**, 272–281.

Burnside, B. & Laties, A. M. 1976 Actin filaments in apical projections of the primate pigmented epithelial cell. *Invest. Ophthal.* **15**, 570–575.

Buyukmhici, N. & Aguirre, G. D. 1976 Rod disc turnover in the dog. *Invest Ophthalmol.* **15**, 579–584.

Chung, S. H., Stirling, R. V. & Gaze, R. M. 1975 The structural and functional development of the retina in larval *Xenopus*. *J. Embryol. exp. Morph.* **33**, 910–940.

Cronly-Dillon, J. R. & Muntz, W. R. A. 1965 The spectral sensitivity of the goldfish and the clawed toad tadpole under photopic conditions. *J. exp. Biol.* **42**, 481–493.

Custer, N. V. 1973 Structurally specialized contacts between the photoreceptors of the retina of the axolotl. *J. comp. Neurol.* **151**, 35–56.

Denton, E. J. & Pirenne, M. H. 1951 The spectral sensitivity of the toad *Xenopus laevis*. *J. Physiol.. Lond.* **115**, 66*P*.

Denton, E. J. & Pirenne, M. H. 1952 Green-coloured rods and retinal sensitivity. *J. Physiol., Lond.* **116**: 33–34*P*.

Denton, E. J. & Pirenne, M. H. 1954 The visual sensitivity of the toad *Xenopus laevis*. *J. Physiol., Lond.* **125**, 181–207.

Deuchar, E. M. 1975 *Xenopus: The south African clawed frog*. London: John Wiley and Sons.

Ditto, M. 1975 A difference between developing rods and cones in the formation of outer segment membranes. *Vision Res.* **15**, 535–536.

Dowling, J. E. & Sidman, R. L. 1962 Inherited retinal dystrophy in the rat. *J. Cell. Biol.* **14**, 73–109.

Dunn, R. F. 1973 The ultrastructure of the vertebrate retina. In *The ultrastructure of sensory organs* (ed. I. Friedman), pp. 153–265. New York: Elsevier Pub. Co.

Fain, G. L., Gold, G. H. & Dowling, J. E. 1976 Receptor coupling in the toad retina. *Cold Spring Harb. Symp. quant. Biol.* XL, 547–561.

Fisher, S. K., Jacobs, G. H., Anderson, D. H. & Silverman, M. S. 1976 Rods in the antelope ground squirrel. *Vision Res.* **16**, 875–877.

Gaze, R. M. 1970 *The formation of nerve connections*. London: Academic Press.

Godfrey, A. J. 1974 The photoreceptors of the chick. Ph.D. dissertation, University of California at Los Angeles.

Gras, W. J. & Worthington, C. R. 1961 X-ray analysis of retinal photoreceptors. *Proc. natn. Acad. Sci. U.S.A.* **63**, 233–238.

Grillo, M. A. & Rosenbluth, J. 1972 Ultrastructure of developing *Xenopus* retina before and after ganglion cell specification. *J. comp. Neurol.* **145**, 131–140.

Hailman, J. P. 1976 Oildroplets in the eyes of adult amphibians: a comparative survey. *J. Morph.* **148**, 453–468.

Hall, M. O., Bok, D. & Bacharach, A. D. E. 1968 Visual pigment renewal in the mature frog retina. *Science, N.Y.* **161**, 787–789.

Hall, M. O., Bok, D. & Bacharach, A. D. E. 1969 Biosynthesis and assembly of the rod outer segment membrane system. *J. molec. Biol.* **45**, 397–406.

Harosi, F. I. 1975 Absorption spectra and linear dischroism of some amphibian photoreceptors. *J. gen. Physiol.* **66**, 357–382.

Hebel, R. 1971 Entwicklung und struktur der retina und des tapetum lucidum des hundes. *Adv. Anat. Embryol. Cell Biol.* **45**, 7–92.

Hogan, M. J., Wood, I. & Steinberg, R. H. 1974 Phagocytosis by pigment epithelium of human retinal cones. *Nature, Lond.* **252**, 305–307.

Hogben, L. 1942 Chromatic behaviour. *Proc. R. Soc. Lond.* B **131**, 111–136.

Hogben, L. & Slome, D. 1936 The pigmentary effector system. *Proc. R. Soc. Lond.* B **120**, 158–173.

Hollyfield, J. G., Besharse, J. C. & Rayborn, M. E. 1976 The effect of light on the quantity of phagosomes in the pigment epithelium. *Expl Eye Res.* **23**, 623–635.

Hunt, R. H. 1975 Developmental programming for retinotectal patterns. *Ciba Fdn Symp.* **29**, 131–159.

Jacobson, M. 1970 *Developmental neurobiology*. New York: Holt, Rinehart & Winston.

Jacobson, M. 1976 Neuronal recognition in the retinotectal system. In *Neuronal recognition* (ed. S. H. Barondes), pp. 2–23. New York: Plenum Press.

Keating, M. J. & Kennard, C. 1976 The amphibian visual system as a model for developmental neurobiology. In *The amphibian visual system* (ed. K. V. Fite), pp. 267–315. New York: Academic Press.

Kinney, M. S. 1977 The photoreceptors and pigment epithelium of the adult and developing *Xenopus* retina: morphology and outer segment renewal. Ph.D. dissertation, University of California at Santa Barbara.

Kinney, M. S. & Fisher, S. K. 1978*a* The photoreceptors and pigment epithelium of the larval *Xenopus* retina: morphogenesis and outer segment renewal. *Proc. R. Soc. Lond.* B **201**, 149–167.

Kinney, M. S. & Fisher, S. K. 1978*b* Changes in length and disk shedding rate of *Xenopus* rod outer segments associated with metamorphosis. *Proc. R. Soc. Lond.* B **201**, 169–177.

Lanzavecchia, G. 1960 Ultrastruturra dei coni e dei bastoncelli nella retina di *Xenopus laevis*. *Archo. ital. Anat. Embriol.* **65**, 417–435.

LaVail, M. M. 1973 Kinetics of rod outer segment renewal in the developing mouse retina. *J. Cell Biol.* **58**, 650–661.

LaVail, M. M. 1976 Rod outer segment disc shedding in rat retina: relationship to cyclic lighting. *Science, N.Y.* **194**, 1071–1074.

Liebman, P. A. & Entine, G. 1968 Visual pigments of frog and tadpole (*Rana pipiens*). *Vision Res.* **8**, 761–775.

Lolley, R. N. & Schmidt, S. Y. 1974 Metabolism of the vertebrate retina. In *The eye: comparative physiology* (eds H. Davson & L. T. Graham), vol. 6, pp. 343–378. New York: Academic Press.

Marks, W. B. (1965) Visual pigments of single goldfish cones. *J. Physiol., Lond.* **178**, 14–32.

Montal, M. & Korenbrot, J. I. 1976 Rhodopsin in cell membranes and the process of phototransduction. In *The enzymes of biological membranes: electron transport and receptors* (ed. A. Martonosi), vol. 4, pp. 365–405. New York: Plenum Press.

Muntz, W. R. A. 1967 The spectral sensitivity of the clawed frog, *Xenopus laevis*. *J. Physiol., Lond.* **189**, 38-49*P*.

Murray, R. L. & Dubin, M. W. 1975 The occurrence of actin like filaments in association with migrating pigment granules in frog pigment epithelium. *J. Cell Biol.* **64**, 705–710.

Nilsson, S. E. G. 1964 An electron microscopic classification of the retinal receptors of the leopard frog (*Rana pipiens*). *J. ultrastruct. Res.* **10**, 390–416.

Nilsson, S. E. G. 1965 The ultrastructure of the receptor outer segments in the retina of the leopard frog (*Rana pipiens*). *J. ultrastruct. Res.* **12**, 207–231.

Porter, K. R. & Yamada, E. 1960 Studies on the endoplasmic reticulum. V. Its form and differentiation in the pigment epithelial cells of the frog retina. *J. Biophys. Biochem. Cytol.* **8**, 181–205.

Rodieck, R. W. 1973 *The vertebrate retina*. San Francisco: W. H. Freeman & Co.

Saxén, L. 1954 The development of the visual cells. *Suomal. Tiedeakat. Toim. (Sarja IV: Biologica)* **23**, 1–107.

Silver née Strange, P. H. 1963 Two spectral sensitivity curves of *Xenopus laevis* obtained by using the melanophore response to light on white and black backgrounds. *J. Physiol., Lond.* **169**, 1–9.

Steinberg, R. H. & Wood, I. 1975 Clefts and microtubules of photoreceptor outer segments in the retina of the domestic cat. *J. ultrastruct. Res.* **51**, 397–403.

Steinberg, R. H., Wood, I. & Hogan, M. J. 1977 Pigment epithelial ensheathment and phagocytosis of extrafoveal cones in human retina. *Phil. Trans. R. Soc. Lond.* B **277**, 459–474.

Stell, W. K. & Harosi, F. I. 1976 Cone structure and visual pigment content in the retina of the goldfish. *Vision Res.* **16**, 647–657.

Stewart, M. M. 1967 *Amphibians of the Malawi state*. New York: University Press.

Witkovsky, P., Gallin, E., Hollyfield, J. G., Ripps, H. & Bridges, C. D. B. 1976 Photoreceptor thresholds and visual pigment levels in normal and vitamin A-deprived *Xenopus* tadpoles. *J. Neurophysiol.* **39**, 1272–1287.

Yamada, E. 1969 The fine structure of the pigment epithelium in the turtle eye. In *The structure of the eye* (ed. G. K. Smelser), pp. 73–84. New York: Academic Press.

Young, R. W. 1967 The renewal of photoreceptor cell outer segments. *J. Cell Biol.* **33**, 61–72.

Young, R. W. 1969 A difference between rods and cones in the renewal of outer segment protein. *Invest. Ophthal.* **8**, 222–231.

Young, R. W. 1970 Visual cells. *Sci. Am.* **223**, 81–91.

Young, R. W. 1971*a* An hypothesis to account for a basic distinction between rods and cones. *Vision Res.* **11**, 1–5.

Young, R. W. 1971*b* The renewal of rod and cone outer segments in the rhesus monkey. *J. Cell Biol.* **49**, 303–318.

Young, R. W. 1974 Biogenesis and renewal of visual cell outer segment membranes. *Expl. Eye Res.* **18**, 215–223.

Young, R. W. 1976 Visual cells and the concept of renewal. *Invest. Ophthal.* **15**, 700–725.

Young, R. W. & Bok, D. 1969 Participation of the retinal pigment epithelium in the rod outer segment renewal process. *J. Cell Biol.* **42**, 392–403.

Young, R. W. & Droz, B. 1968 The renewal of protein in retinal rods and cones. *J. Cell Biol.* **39**, 169–184.